



Zabbarova, I. V., Ikeda, Y., Carder, E. J., Wipf, P., Wolf-Johnston, A. S., Birder, L. A., Yoshimura, N., Getchell, S. E., Almansoori, K., Tyagi, P., Fry, C. H., Drake, M. J., & Kanai, A. J. (2018). Targeting p75 neurotrophin receptors ameliorates spinal cord injury-induced detrusor sphincter dyssynergia in mice. *Neurourology and Urodynamics*.
<https://doi.org/10.1002/nau.23722>

Peer reviewed version

License (if available):
Unspecified

Link to published version (if available):
[10.1002/nau.23722](https://doi.org/10.1002/nau.23722)

[Link to publication record in Explore Bristol Research](#)
PDF-document

This is the author accepted manuscript (AAM). The final published version (version of record) is available online via Wiley at <https://onlinelibrary.wiley.com/doi/10.1002/nau.23722>. Please refer to any applicable terms of use of the publisher.

University of Bristol - Explore Bristol Research

General rights

This document is made available in accordance with publisher policies. Please cite only the published version using the reference above. Full terms of use are available:
<http://www.bristol.ac.uk/red/research-policy/pure/user-guides/ebr-terms/>

Targeting p75 neurotrophin receptors ameliorates spinal cord injury-induced detrusor sphincter dyssynergia in mice

Irina Zabbarova¹, Youko Ikeda¹, Evan Carder², Peter Wipf², Amanda Wolf-Johnston¹,
Lori Birder^{1,3}, Naoki Yoshimura^{3,4}, Samuel Getchell¹, Khalifa Almansoori¹, Pradeep
Tyagi⁴, Christopher Fry⁵, Marcus Drake⁵ and Anthony Kanai^{1,3}

1. University of Pittsburgh, Department of Medicine, Renal-Electrolyte Division
2. University of Pittsburgh, Department of Chemistry
3. University of Pittsburgh, Department of Pharmacology and Chemical Biology
4. University of Pittsburgh, Department of Urology
5. University of Bristol, School of Physiology, Pharmacology and Neuroscience

Corresponding author:

Anthony Kanai, Ph.D., University of Pittsburgh

A1224 Scaife Hall, 3550 Terrace Street, Pittsburgh, PA 15261 USA

Email: ajk5@pitt.edu; Tel: 412-624-1430

Keywords: LM11A-31, lower urinary tract dysfunction/symptoms (LUTD/LUTS);
neurodegeneration, neurogenic bladder dysfunction, proneurotrophins.

Running title: LM11A-31 treats DSD

Abstract

Aims: To determine the role of p75 neurotrophin receptor (p75^{NTR}) and the therapeutic effect of the selective small molecule p75^{NTR} modulator, LM11A-31, in spinal cord injury (SCI) induced lower urinary tract dysfunction (LTUD) using a mouse model.

Methods: Adult female T₈-T₉ transected mice, were gavaged daily with LM11A-31 (100 mg/kg) for up to 6 weeks, starting one day before or seven days following injury. Mice were evaluated *in vivo* using urine spot analysis, cystometrograms (CMGs) and external urethral sphincter (EUS) electromyograms (EMGs); and *in vitro* using histology, immunohistochemistry and western blot.

Results: Our studies confirm the expression of p75^{NTRs} in mouse bladder and dorsal horn of the lumbar-sacral (L₆-S₁) spinal cord which significantly decreased following SCI. LM11A-31 prevented or ameliorated the detrusor sphincter dyssynergia (DSD) and detrusor overactivity (DO) in SCI mice, significantly improving bladder compliance. Furthermore, LM11A-31 treatment blocked the SCI-related urothelial damage and bladder wall remodeling.

Conclusion: Drugs targeting p75^{NTRs} can moderate DSD and DO in mice, may identify pathophysiological mechanisms and have therapeutic potential in SCI patients.

Introduction

Detrusor Sphincter Dyssynergia. Storage and emptying of urine from the bladder are dependent on coordinated contraction/relaxation of the smooth and striated muscles in lower urinary tract organs mediated by neural circuitry in the brain and spinal cord¹. During storage, detrusor smooth muscle is relaxed, while the smooth and striated muscles of external urethral sphincter (EUS) contract to maintain continence. The converse happens during micturition, when the detrusor smooth muscle contracts and the EUS relaxes. This voluntary control of micturition is lost following spinal cord injury (SCI) rostral to the lumbosacral spinal segments, and the bladder becomes areflexic. Following recovery from spinal shock, reflex bladder activity re-emerges with the formation of a spinal micturition pathway, and ultimately the bladder becomes hyperreflexic². SCI also leads to detrusor sphincter dyssynergia (DSD) which describes the simultaneous contraction of the bladder and EUS. DSD is commonly attributed to the interruption of descending inhibitory pathways from the pontine micturition center (PMC) to EUS motoneurons in Onuf's nuclei within the sacral spinal cord. Various therapies have been employed to reduce DSD; however, the results have failed to satisfy the Level 1 recommendation³. DSD causes urinary retention—a major problem in the care of SCI patients. The resultant high intravesical pressures can induce ureteral reflux and potentially lead to renal failure.

Detrusor Overactivity (DO). Urinary retention, bladder distention and inflammation, secondary to DSD-induced outlet obstruction, lead to bladder wall hypertrophy and DO, where the latter has neurogenic and myogenic components. Neurogenic detrusor overactivity (NDO) results from neural remodeling and afferent sensitization, whereas

myogenic DO occurs due to a combination of increased coupling of putative pacemaker interstitial cells and detrusor smooth muscle and stretch-evoked urothelial ATP release⁴. Increased myogenic activity may also stimulate mechanosensitive afferents⁵ to trigger reflex bladder contractions and exacerbate NDO symptoms.

Neurotrophic factors and p75^{NTRs}. Nerve growth factor (NGF) and brain-derived neurotrophic factor (BDNF) are released by detrusor smooth muscle, mast cells and urothelial cells in various pathologies⁶. Mature NGF and BDNF are enzymatically processed within secretory vesicles from their proneurotrophins (proNGF/proBDNF) before release⁷. During pathology⁸, their overexpression exceeds the rate of processing leading to unregulated release of proneurotrophins which differ from mature forms in their affinity for p75^{NTRs}, the expression of which is increased following SCI in the bladder and neuronal pathways governing micturition⁹. Furthermore, proNGF/proBDNF preferentially activate the p75^{NTR}-sortilin complex. Sortilin is transport protein involved in the organization of intracellular cargo between membrane compartments, that when activated by proneurotrophins in conjunction with p75^{NTR} can induce apoptosis in many cell types¹⁰. The mature neurotrophins activate their cognate tropomyosin receptor kinase (Trk) and p75^{NTR} heterodimer, promoting survival and differentiation (Figure 1A).

Upon proneurotrophin binding, full-length p75^{NTRs} undergo proteolytic cleavage, removing the extracellular domain (ECD) and leaving the membrane bound carboxyl-terminal fragment. Further cleavage generates the soluble intracellular domain (ICD), which can translocate to the nucleus¹¹, activating apoptotic transcriptional targets in addition to pathways activated by the full-length p75^{NTR}¹⁰.

LM11A-31 and LM11A-24. These are small organic molecules identified as modulators of p75^{NTRs} through *in silico* screening for potential to mimic the binding activity of the loop 1 domain of NGF and competitively antagonize proneurotrophin binding¹². However, these molecules can also have the potential to directly activate p75^{NTR} associated signaling¹³. LM11A-31 partitions mostly to the CNS and has been shown to improve motor coordination after spinal cord contusion injury in mice¹⁴. The absence of toxicity or exacerbation of injury-associated pain¹⁴ in previous studies using LM11A-31 affirms its possible therapeutic potential for treating neurogenic LUTD. Therefore, our aim was to determine the effect of oral administration of LM11A-31 on LUTD in a thoracic SCI mouse model.

Methods

SCI surgery (T₈-T₉ transection). SCI surgery was performed as previously described⁵. Briefly, adult female C57BL/6 mice (18-25 g) were anesthetized with isoflurane (5% induction/1.5% maintenance) and a laminectomy performed at the T₈-T₉ spinal level. The cord was completely transected, the resultant space between the cut ends filled with hemostatic sponge to minimize bleeding and the muscle layer and overlying skin sutured. Subsequently, bladders were expressed by gentle abdominal compression, twice-daily, for one week. The animals were used for experiments one day to six weeks following SCI.

LM11A-31 and LM11A-24 treatment. Both LM11A-31 and LM11A-24 were synthesized in house. Mice were administered once-daily gavage of water (100 µl) in controls and aqueous solutions of LM11A-31 or LM11A-24 (100 mg/kg) in treated groups.

Treatment was initiated either a day before or seven days after SCI, until experimental endpoints. Spinal cord intact mice were also administered the drugs or vehicle for a seven day period, a week following SCI.

Histology. Mice were sacrificed according to the University's Institutional Animal Care and Use Committee approved methods, urinary bladders dissected and opened longitudinally along the ventral aspect, flattened, fixed overnight in 10% paraformaldehyde, embedded in paraffin, sectioned transversely (3 μ m) and stained with hematoxylin and eosin or 2% acidified toluidine blue (mast cell stain) for light microscopy.

Enzyme linked immunosorbent assay (ELISA). Urine samples were collected from the bladders of mice immediately following euthanasia using a 32-gauge insulin syringe, and immediately frozen on dry ice and stored at -80°C. Levels of p75^{NTR} ECD were evaluated using a mouse NGFR/p75^{ECD} rapid ELISA kit (Biosensis) according to manufacturer instructions.

Western blotting. The mucosa and detrusor muscle layers were separated by blunt dissection, and samples were homogenized (Lysing Matrix D using FastPrep-24, MP Biomedicals) in Hank's balanced salt solution containing complete protease inhibitor cocktail (1 tablet/10 ml, Roche) and phosphatase inhibitor cocktail (Sigma, 1:100). After centrifugation (10,000 x g; 15 min at 4°C), the supernatant was collected, and the membrane protein fraction was prepared by suspending pellets in lysis buffer (0.3 M NaCl, 50 mM Tris-HCl pH7.6 and 0.5% Triton X-100) with protease/phosphatase inhibitors as above. Supernatants were pooled for whole cell lysates and protein concentrations determined using a BCA protein assay (Pierce). After denaturation (100°C for 5 min) in Laemmli sample buffer, 40 μ g of each lysate was separated on a 4-

15% TGX Stain-Free SDS-PAGE gel (Bio-Rad). Proteins were transferred to PVDF membranes and incubated overnight at 4°C with primary antibodies against the ICD of p75^{NTR}, proNGF, proBDNF and β -actin (details of antibodies in supplemental figure 13) diluted in Tris-buffered saline with 0.1% Tween-20 (TBS-T) containing 5% (w/v) milk. Membranes were incubated with appropriate horseradish peroxidase conjugated secondary antibodies in 5% (w/v) Milk TBS-T, washed, and incubated in WesternBright Quantum (Advansta) for chemiluminescent imaging (ChemiDoc MP, Bio-Rad). Optical density of each protein species was normalized to total protein levels using Image Lab software (Bio-Rad).

Immunofluorescence. Whole bladders and spinal cord segments were isolated, embedded in optimal cutting temperature medium and frozen on dry ice (n=3 per group). The bladders were sectioned (10 μ m) on a cryostat and immediately processed for immunofluorescent detection of p75^{NTRs}, tyrosine hydroxylase (TH) and calcitonin gene related protein (CGRP) using a previously described protocol¹⁵. The p75^{NTR} expression and p75^{NTR}-CGRP/TH colocalization analysis were performed using ImageJ (NIH) and MATLAB (MathWorks Inc.) software, respectively.

Urine spot assay. Mice were placed individually in clean metabolic cages lined with Whatman filter paper at the bottom for two hours, between 11 a.m. and 2 p.m., with water and food withheld for the duration of the assay. The filter papers were visualized under UV light, images retained as TIFF files and analyzed using ImageJ software using a previously described method¹⁶ (see supplemental figure 8).

Transepithelial resistance (TER) measurements. Following euthanasia, bladders were excised, washed with oxygenated Ringer's solution, opened to form a sheet,

mounted on a nylon ring (0.09 cm² exposed area) and placed in Ussing chambers under constant oxygenation and temperature control. TER was determined by passing current through Ag/AgCl electrodes and measuring the voltage deflection (V_t) with another pair of electrodes. Data were digitized for display, analysis and storage.

Decerebrate CMG and EMG recordings. Mice were anesthetized using isoflurane and an incision made in the neck to expose the carotid arteries and trachea. Ligatures were placed around the carotids to decrease cerebral blood flow and a tracheotomy performed using PE-60 tubing. After a craniotomy, the brain rostral to the supracollicular level was sectioned. Decerebration allowed cystometric assessment to be performed without anesthetics which can block reflex bladder contractions. A PE-50 catheter was inserted through the bladder dome, secured using a suture and connected to a pressure transducer and syringe pump. Two stainless steel 50 μ m electrodes were inserted transperineally 1 mm lateral to the urethra to record EUS activity. The bladder was emptied manually and then filled with saline at 0.01 ml/min until reflex contractions were elicited to perform voiding cystometry.

Statistical Analysis. Quantitative data are shown as mean \pm SD. One and two-way ANOVA was used to determine between group differences with Tukey's multiple comparisons test, differences between data sets were tested with unpaired Student's t -test, and skewed data sets with a Mann-Whitney U test; significance was $p < 0.05$.

Study Approval. All animal procedures were compliant with the National Institutes of Health "Guide for the Care and Use of Laboratory Animal" and received institutional ethical approval.

Results

LM11A-31 improves voiding efficiency. *In vivo* voiding patterns were assessed using urine spot test analysis over a two-hour period (Figure 2 and Supplemental Figure 7). Spinal cord intact mice were continent and voided in one area of the cage (Figure 2A). Voiding patterns and voided volumes of spinal cord intact mice were not affected by daily administration of LM11A-24 (Figure 2B) or LM11A-31 (Figure 2C), the maximal dosage shown to improve motor recovery following spinal cord contusion injury¹⁴. Two weeks post-SCI, mice exhibited random urine spots and a significant decline in voided volumes (Figure 2D). Daily treatment with the peripherally acting LM11A-24¹⁷ did not affect these parameters (Figure 2E), but the centrally acting LM11A-31 significantly increased the voided volumes ($p < 0.05$ compared to vehicle treated SCI mice, Student's *t*-test), indicating improvement in voiding efficiency (Figure 2F). A table listing the spot test voided volumes and calibration data are shown in Supplemental Figures 7 and 8.

LM11A-31 ameliorates DSD and NDO. The effects of targeting p75^{NTR} inhibition on bladder and EUS function were assessed by decerebrate CMG and EUS-EMG measurements. Spinal cord intact mice showed long intercontractile intervals and low filling pressures (Figure 3A) along with EUS bursting and reduction of tonic sphincter activity during voiding (Figure 3A-1). At two weeks post-SCI, there was a loss of regular micturition patterns, emergence of nonvoiding contractions (*i.e.* DO) and increased EUS tonic activity with decreased bursting in response to bladder contractions, *i.e.*, DSD (Figures 3B, B-1). Daily treatment with LM11A-31 initiated one week following SCI reduced nonvoiding bladder contractions, decreased concurrent EUS tonic activity and increased bursting to improve voiding efficiency (Figures 3C, C-1). The amelioration of

DO and DSD was accompanied by a significant increase in bladder compliance. Daily LM11A-31 prevented the development of NDO in the experimental assessments at the six week timepoint (Figures 3D-F). Data tables for CMG and EMG recordings are shown in supplemental figures 9 and 10.

LM11A-31 preserves urothelial structure and barrier function. SCI resulted in acute disruption of the urothelium (Figures 4B vs. A). When mice were administered LM11A-31 starting one day pre-surgery, bladders showed protection against SCI-induced urothelial loss (Figure 4C). At 10 days post-SCI, further morphological changes to the bladder were manifested as hyperplasia of the urothelium and lamina propria as well as detrusor hypertrophy (Figure 4D). These changes were prevented by daily LM11A-31 treatment (Figure 4E). The loss of barrier function in SCI animals was apparent from a significant reduction of transepithelial resistance (TER) and this adverse event was prevented by administration of either LM11A-24 or LM11A-31 initiated prior to SCI (Figure 4F). Toluidine blue staining demonstrated that the numbers of activated mast cells in SCT bladders two weeks following injury were significantly greater than in control uninjured bladders (8.1 ± 1.6 cells/mm² versus 1.4 ± 1.6 cells/mm², respectively, $p < 0.01$, unpaired Student's *t*-test). Daily treatment with LM11A-31 initiated one day before SCI significantly decreased the mast cell numbers (3.2 ± 1.7 cells/mm², $p < 0.01$ versus untreated SCI). LM11A-24 treatment also decreased the number of activated mast cells, but less significantly (6.5 ± 2.2 cells/mm², $p = 0.05$ versus untreated SCI).

Alteration in p75^{NTR} and proneurotrophin levels in the urine and urinary bladder following SCI. Urine levels of p75^{NTR} ECD were evaluated by ELISA, one to seven days following SCI (Figure 4G). A sharp rise in p75^{NTR} ECD levels noted one day post-injury,

was decreased by LM11A-31 pretreatment, SCI-induced elevations of the p75^{NTR} ECD were observed at much lower levels for up to seven days post-injury.

Western blot analysis showed full-length p75^{NTRs} are more highly expressed in the detrusor than the mucosa and these levels are decreased at seven days post SCI. LM11A-31 treatment blocked the loss of p75^{NTR} expression in SCI animals (Figure 4H and I). LM11A-31 treated mice had elevated proBDNF levels compared to untreated SCI and control mice. The protein level of proNGF was not significantly different in the mucosa or detrusor samples from control, SCI and SCI + LM11A-31 groups (data not shown). The p75^{NTR} and proBDNF levels normalized to β -actin are summarized in the bar graphs in Figure 4I.

Expression of p75^{NTRs} on TH- and CGRP-positive nerve fibers in bladder and spinal cord segments. In spinal cord intact mice, p75^{NTRs} were found throughout the bladder wall and colocalized with TH- ($6.1 \pm 3.7\%$ of p75^{NTR} labeling in bladder wall) and CGRP-positive ($8.3 \pm 1.8\%$ of p75^{NTR} labeling in bladder wall) nerve fibers (Figures. 5A, D, J, K and L). There was no detectable p75^{NTR} labeling on cholinergic nerves or fibroblasts (not shown). At seven days post-SCI, p75^{NTR} expression decreased in the detrusor layer ($6.9 \pm 1.9\%$ of detrusor area in controls *versus* $3.7 \pm 1.8\%$ in SCI) while maintaining a similar degree of colocalization with TH- or CGRP-positive nerves; $3.1 \pm 1.8\%$ and $6.4 \pm 1.8\%$ colocalization with p75^{NTR}, respectively. (Figures 5B, E, J and K) There was also increased expression in basal/intermediate urothelial cells which was not observed in spinal cord intact mouse bladders (Figure 5L and M). Daily LM11A-31 treatment of SCI mice did not significantly alter total p75^{NTR} expression in the urothelium or detrusor, nor the colocalization of p75^{NTR} with CGRP or TH compared to untreated SCI

mice (Figure 5J and K). The % area of p75^{NTR} expression in the urothelium did not differ between spinal cord intact (1.2 ± 0.6 %), SCI (2.3 ± 2.3 %) and SCI mice with LM11A-31 (1.4 ± 1.3 %) or LM11A-24 (2.2 ± 0.8 %) treatment. In control mice, expression of p75^{NTR} in L₆-S₁ spinal cord segment was limited to the dorsal horn (45.0 ± 11.0 % of dorsal horn area) with the highest density in the lamina-II region (Figure 5G). At seven days post-SCI, there was a significant decrease in p75^{NTR} expression in the lamina-II region of the dorsal horn (from 77.8 ± 16.8 % in controls to 44 ± 19.6 % of lamina-II area) (Figure 5H), which was not altered by LM11A-31 treatment (42.0 ± 3.7 %) (Figure 5I).

Discussion

SCI-induced LUTD is described by the symptoms and signs including DSD, NDO, myogenic DO, and urothelial barrier disruption, hypertrophy and hyperplasia. These physiological and histological changes correlate with increased production of proNGF/proBDNF by denervated tissues within the spinal cord and bladder wall following SCI¹⁸.

The expression of p75^{NTRs} is previously reported to be localized in urothelium of rat bladders¹⁹ and in SCI patient biopsies⁹, where p75^{NTRs} likely contribute to the urothelial injury in SCI. Our study suggests that under normal conditions, there is robust expression of p75^{NTRs} in the urinary bladder where a select population colocalize with CGRP and TH-positive innervating the mouse urothelium and detrusor (Figures 5A, D and K) some of which could potentially originate from bladder innervating neurons in L1 and S1 dorsal root ganglia (supplemental figure 11). LM11A-31 treatment did not affect the decrease in p75^{NTR} or the % colocalization with TH or CGRP, suggesting this drug may be altering

functional properties of bladder nerves to bring about their therapeutic effect. SCI have been shown to enhance bladder sensory neuron firing due to increased Na⁺ channel currents density and a similar effect has been demonstrated with chronic intrathecal NGF administration². The effect of LM11A-31 on bladder afferent firing has yet to be determined, however, our data show that treatment can ameliorate SCI-induced DO and significantly improve bladder compliance, suggesting an effect on afferent activity. Following SCI, there is increased p75^{NTR} expression in the basal/intermediate urothelium (Figure 5M) which could correlate with proliferating cells found during the first seven days after SCI²⁰. This suggests neurotrophin signaling may be involved in maintaining urothelial differentiation or regeneration of the urothelium following injury. Strong p75^{NTR} expression is also noted in the dorsal horn of L₆-S₁ spinal cord segments (Figure 5G), as reported previously²¹. The high level of p75^{NTR} in the detrusor layer noted in western blots (Figure 4H-I) could be due to higher density of p75^{NTR} positive nerve fibers compared to the mucosa (Figure 5). Studies with urothelial NGF overexpressing mice²² also showed enhanced expression of p75^{NTR} in the detrusor layer compared to control mouse bladders. Our data demonstrate that p75^{NTR} ECD fragments are elevated in acute SCI (Figure 4G), suggesting that binding of proneurotrophins is inducing the p75^{NTR} cleavage. However, we cannot rule out that some of the ECD protein excreted in the urine may be contributed by other organs/tissues. Pretreatment with LM11A-31 blocked the rise of urinary p75^{NTR} ECD levels that occurs within 24 hours of SCI, suggesting LM11A-31 treatment in the clinical setting may be most beneficial within hours following SCI to prevent the activation of neurodegenerative pathways. Nonetheless, we have also demonstrated that LM11A-31 ameliorated DSD and DO when given one week following

SCI (Figure 3C). Our data showed a significant decline in measurable amounts of proBDNF by seven days post-SCI and this decline was not observed in LM11A-31 treated groups (Figure 4I) suggesting displacement of proBDNF by LM11A-31 raises the levels of free proBDNF. This trend was not observed with proNGF, whose production in bladder was lower than proBDNF (not shown). There may be multiple factors (e.g. inflammation induced mRNA instability, disruption in protein translation mechanisms) that could be attributed to decreased proneurotrophin levels in SCI. Enhanced uptake and retrograde transport of neurotrophins from the bladder, proposed for changes in NGF levels following SCI²³, could potentially be involved. As LM11A-31 treatment prevented the decline in proBDNF, it suggests the drug is preventing proneurotrophin binding and subsequent transport, supporting the concept of SCI-induced alterations in neurotrophin uptake.

We propose that unregulated release of proNGF/proBDNF from vesicular stores²⁴ stimulates p75^{NTR}-positive nerves and the urothelium to initiate degenerative pathways. The consequent urothelial disruption, urine infiltration and inflammation lead to increased release of excitatory transmitters²⁵ from sensory nerves that further potentiates the inflammatory processes to promote afferent sensitization and exacerbation of NDO. The urothelium shows constitutive expression of NGF which is believed to participate in maintaining normal bladder function²⁵. During the acute phase of SCI, it could be speculated that urothelial disruption and nerve injury causes a rapid increase in neurotrophin expression²³. Our data suggest proneurotrophin signaling predominates within 24 hours following SCI and may be responsible for the detrimental p75^{NTR} signaling in the bladder. At later time points following SCI, there may be proportionally more mature neurotrophins in the bladder than under normal conditions²³ as a compensatory

mechanism to promote nerve growth. Loss of bladder and L6-S1 p75^{NTR} expression in SCI suggests impairment of afferent and efferent function in the bladder precedes the urinary retention noted acutely following injury. Loss of nerve fibers is also noted in bladders of SCI patients²⁶. Activation of p75^{NTR} leads to receptor internalization and retrograde axonal transport to induce transcriptional changes²⁷ and may account for decreased p75^{NTR} expression in the bladder following SCI. LM11A-31 treatment did not change bladder or L6-S1 spinal cord p75^{NTR} expression compared to vehicle treated SCI mice (supplemental figure 12), suggesting it may rather augment sensory nerve activity in the dorsal root ganglia or L3-L4 EUS centers to ameliorate SCI-induced DO and DSD.

The actions of LM11A-31 and LM11A-24 were compared to elucidate the sites of action responsible for the observed effects, because LM11A-31 crosses the blood-brain barrier¹⁴ and may act on the CNS and periphery, whilst LM11A-24 has mainly peripheral actions^{14,17}. Both agents did not alter voiding patterns when given to animals with intact spinal cords (Figures 2B, C). In SCI animals, LM11A-31, but not LM11A-24, was able to ameliorate NDO and DSD and increase voided volumes (Figure 2F and E, respectively and Supplemental Figure 7). However, both LM11A-24 and LM11A-31 could prevent urothelial barrier disruption (Figure 4F), demonstrating a shared peripheral site of action for both ligands. Preventing urothelial disruption may account for the decreased number of activated mast cells in the bladder wall, however, mast cells also express p75^{NTR} and we cannot exclude a direct effect of p75^{NTR} modulators on these cells. We infer that central actions of LM11A-31 are critical for the improvement of DSD and NDO and peripheral actions of the drug may further augment the central effects.

Based on our findings, a description of our hypothesis for the development of SCI-induced DSD and NDO and putative therapeutic sites of action of LM11A-31/24 are shown in supplemental figure 6.

Conclusion

The proposed therapeutic use of LM11A-31 to treat SCI-induced LUTD is clinically relevant as there are currently no pharmacological agents to treat DSD. This agent also has therapeutic effect on NDO, can be administered orally and is safe and has entered phase II clinical trials for Alzheimer's disease²⁸.

Figure legends

Figure 1. Schematics of p75^{NTR} signaling pathways A) The p75^{NTR} signals through dimerization with sortilin or Trk receptors. p75^{NTR}-sortilin complexes will preferentially bind proNGF/proBDNF that activate apoptotic signaling cascades. Conversely, p75^{NTR}-Trk receptors bind to mature neurotrophins to activate cell survival pathways. LM11A-31 is a dual-action drug that can downregulate apoptotic JNK signaling through the p75^{NTR}-sortilin dimer, while promoting activation of AKT-mediated survival pathways through disinhibition and/or activation of the TrkA/B^{NTR}-p75 dimer in UROtsa cells challenged with protease resistant proNGF.

Figure 2. Urine spot analysis and the beneficial effect of LM11A-31 in SCI mice. Tests were conducted on control or SCI mice, receiving vehicle (water) or LM compound (n≥4). A) Normal voiding pattern from a mouse with an intact spinal cord receiving water. B) A control mouse receiving LM11A-24 (100 mg/kg/day). C) A control mouse receiving LM11A-31 (100 mg/kg/day). D) Voiding pattern of a SCI mouse receiving water. E) SCI mouse receiving LM11A-24. F) SCI mouse receiving LM11A-31.

Figure 3. LM11A-31 ameliorates SCI-induced DSD and NDO. A) Control mouse. The inset (A1, right) shows the boxed area of the expanded time-base. B) SCI mouse two weeks post-injury, receiving vehicle (water). C) SCI mouse receiving LM11A-31 starting one week post-SCI (n≥4). D) SCI mouse receiving LM11A-24 starting one week post-SCI. E) Control mouse, CMG recording. F) SCI mouse six weeks post-injury,

receiving vehicle (water). G) SCI mouse six weeks post-injury, receiving LM11A-31 starting from the day prior to injury.

Figure 4. Pretreatment with LM11A-31 or -24 prevents SCI-induced adverse morphological changes in the bladder wall. A) H&E stained section of a control mouse bladder. B) Bladder section of a SCI mouse (one day post-injury) receiving water. C) Bladder section of a SCI mouse (one day post-injury) administered LM11A-31. D) Bladder section of a SCI mouse (10 days post-injury) receiving water. E) Bladder section of a SCI mouse bladder (10 days post-injury) receiving LM11A-31. (A. – E., $n \geq 3$). F) Value of TER in bladder wall sheets from control and SCI mice (one day post-injury) with or without LM11A-31 or LM11A-24 treatment. All treatments commenced one day prior to injury. Mean data \pm SD; $p < 0.05$ vs. control ($n \geq 4$, unpaired Student's *t*-test). G) $p75^{\text{NTR}}$ ECD levels measured by ELISA (Biosensis) from mouse urine. These values dramatically increased one day following SCI (*, $p < 0.05$, $n = 4$) in comparison to control animals ($n = 6$). At this time point, pretreatment with LM11A-31 significantly decreased the amount of cleaved $p75^{\text{NTR}}$ ECD (**, $p < 0.05$, $n = 4$). The $p75^{\text{NTR}}$ ECD levels measured three days post-transection, were comparatively lower, and the levels were sustained until seven days post-injury. The LM11A-31 treatment decreased the sustained $p75^{\text{NTR}}$ ECD levels in the urine at three and seven days following SCI. H) Western blot analysis of $p75^{\text{NTRs}}$, proBDNF and β -actin in the mucosa and detrusor of control, SCI and LM11A-31 treated mice seven days post-injury. The full-length $p75^{\text{NTR}}$ protein (75 kDa band) was highest in control samples and significantly decreased in both mucosa and detrusor layers following SCI. Daily treatment with LM11A-31 prevented the decrease in full-length

p75^{NTR}. The antibody used for p75^{NTR} detection also detected multiple smaller weight bands resulting from proteolytic cleavage following receptor activation. I) Relative expression of p75^{NTR} and proBDNF normalized to β -actin. * $p < 0.05$, *versus* control samples.

Figure 5. Immunofluorescent labelling of p75^{NTRs}, their colocalization with Calcitonin Gene-Related Peptide (CGRP) and Tyrosine Hydroxylase (TH)-positive nerves – effect of LM11A-31. A) p75^{NTRs} (green) were expressed on TH-positive structures (red) in spinal cord (SC) intact mouse bladders. B) Seven days post-SCI. C) p75^{NTRs} and their colocalization with TH-positive nerves was present in bladders of SCI mice (seven days post-injury) pretreated with LM11A-31. The colocalization between SC intact, SCI and SCI with LM11A-31 treatment were not significantly different; $p > 0.05$, One-way ANOVA with Tukey's multiple comparison test. D) p75^{NTRs} also colocalized with bladder CGRP-positive nerves (red) in SC intact animals. Colocalization is indicated by merged yellow fluorescence and highlighted with yellow arrows. E) Seven days post-SCI: p75^{NTR}-immunoreactivity (green) decreased compared to SC intact mice, the % area colocalized with CGRP (red) did not significantly change. F) Expression level of p75^{NTR} and colocalization of p75^{NTRs} with CGRP-positive nerves was not found to differ from vehicle treated SCI mice (DT = detrusor; LP = lamina propria; and UT = urothelium). G) p75^{NTR} expression localized to the dorsal horn (white outlined region) of L₆-S₁ spinal cord segments in SC intact mice. H) p75^{NTR} labeling in seven day post-SCI mouse with decreased expression in lamina-II region. I) SCI mice with LM11A-31 for seven days. J) Colocalization analysis of p75^{NTR} CGRP and K) TH immunofluorescence. The % area that overlapped between p75^{NTR} and CGRP or p75^{NTR} and TH immunofluorescence were

quantified using MATLAB software within the total bladder wall area as defined by DAPI staining. L) p75^{NTR} and CGRP expressing fiber in SC intact mouse urothelium (white bordered region). M) p75^{NTR} expression in urothelial basal layer of SCI mouse bladders which was not found in SC intact mice. Similar urothelial staining profile was also seen with SCI + LM11A-31 and SCI + LM11A-24 treated mice. Graphical representation of % area expression of p75^{NTR} in the bladder wall and L6-S1 dorsal horn are shown in supplemental figure 12.

Supplemental figure 6. Mechanisms of proneurotrophins in SCI-induced LUTD and amelioration by LM11A-31 and -24. A) The p75^{NTR} signals through dimerization with sortilin or Trk receptors. p75^{NTR}-sortilin complexes will preferentially bind proNGF/proBDNF that activate apoptotic signaling cascades. Conversely, p75^{NTR}-Trk receptors bind to mature neurotrophins to activate cell survival pathways. Table 1) Neurotrophin receptors and their ligands. B-C) Schematic of neural connections that regulate voiding and the alterations following SCI that contribute to DSD and bladder dysfunction). B) Under normal conditions, the urinary bladder and EUS receive parasympathetic inputs from the L₆-S₁ spinal cord *via* pelvic and pudendal nerves, respectively. These inputs are regulated by supraspinal sites to coordinate afferent input [1] to the PMC that results in outflow to parasympathetic neurons [2] for bladder contraction and activation of inhibitory neurons [3] that act on motoneurons in Onuf's nuclei to relax the EUS. In rodents, there are also inhibitory interneurons in the L₃-L₄ region that project to Onuf's nuclei to promote EUS bursting [4] and death of these inhibitory interneurons may contribute to the development of DSD. C) Data in Figure 5G-

I demonstrate the selective expression of p75^{NTRs} in the dorsal horn of a mouse L₆ spinal cord segment whose selective stimulation by LM11A-31 leads to the remodelling that we hypothesize includes afferent projections to parasympathetic efferent nerves [5] that accounts for the bladder to spinal cord reflex. We propose that the action of LM11A-31 on cell pro survival signaling pathways allows it to promote growth of afferent projections to the L₃-L₄ region [7] and preserve the survival of inhibitory neurons in the L₃-L₄ region to alleviate DSD. [8] LM11A-31 prevents proneurotrophin binding to p75^{NTRs} on sympathetic and sensory nerve endings in the bladder wall, to prevent urothelial disruption and afferent sensitization and the development of NDO, respectively.

Supplemental Figure 7. Voided volumes calculated from spot tests using ImageJ.

Supplemental Figure 8. Calibration data for spot test analysis.

Supplemental Figure 9. Values of pressure threshold (PT), maximal voiding pressure (MVP), baseline pressure (BP), intercontraction intervals (ICI), bladder compliance (BC), the number of nonvoiding contractions (NVC), voided volumes (VV) and residual volumes (RV) from cystometric recordings represented in figure 3 (n≥4). (*p<0.05 compared to control group, unpaired Student's *t*-test).

Supplemental Figure 10. Values of contraction duration (CD), voiding duration (VD) and EUS bursting activity in control, 2 weeks SCI and 2 weeks SCI with LM11A-31

therapy started a week following injury ($n \geq 4$). ($*p < 0.01$ compared to both control and 2 weeks SCI with LM11A-31 therapy, unpaired Student's t -test).

Supplemental Figure 11. Coexpression of p75^{NTR} and TH or CGRP in DRG neurons innervating the mouse urinary bladder. Bladders of SC intact mice were injected with 10 μ l of 2% fast blue solution and L1 and S1 DRG were isolated after one week and examined for expression of p75^{NTR} and TH or CGRP on bladder specific sensory neurons by immunofluorescence. A) p75^{NTR} and TH were found to colocalize on neurons in L1 DRG which send projections to the bladder through the hypogastric nerve (white arrows). B) S1 DRG (that send projections *via* pelvic nerve) also showed a small number of fast blue labeled sensory neurons that colocalized with p75^{NTR} and TH (white arrow). These indicate that some p75^{NTR} + TH-positive fibers in the bladder could be from sensory neurons. In C) L1 DRG and D) S1 DRG, p75^{NTR} and CGRP were found to colocalize on fast blue labeled neurons (white arrows).

Supplemental Figure 12. Quantification of p75^{NTR} expression in the urothelial and detrusor layers and L6-S1 spinal cord segment. The percentage area of p75^{NTR} immunofluorescence was quantified using ImageJ software in urothelial, detrusor and dorsal horn region. Labeling in the urothelial layer was not significantly altered in control, SCI, and treatment groups. p75^{NTR} levels significantly decreased in the detrusor layer following SCI ($*p < 0.05$ compared to SC intact, Two-way ANOVA with Tukey's multiple comparisons test). LM11A-31 or LM11A-24 treatment in SCI mice did not alter detrusor layer p75^{NTR} expression compared to vehicle treated SCI mice. The L6-S1 spinal cord

p75^{NTR} expression was decreased in lamina-II region (**p<0.001 compared to SC intact, Two-way ANOVA with Tukey's multiple comparisons test) and did not change with LM11A-31 treatment.

Supplemental figure 13. Table of antibodies used for immunofluorescence and western blots.

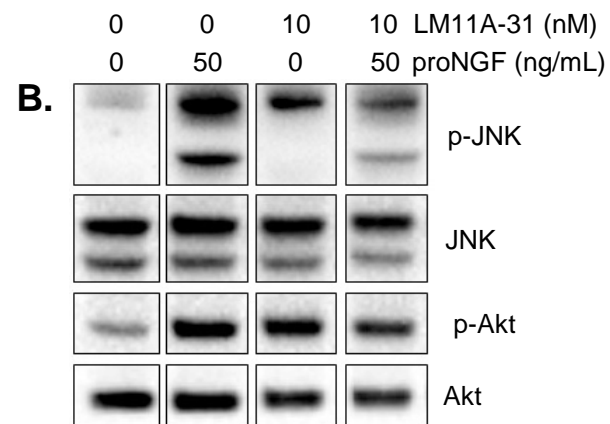
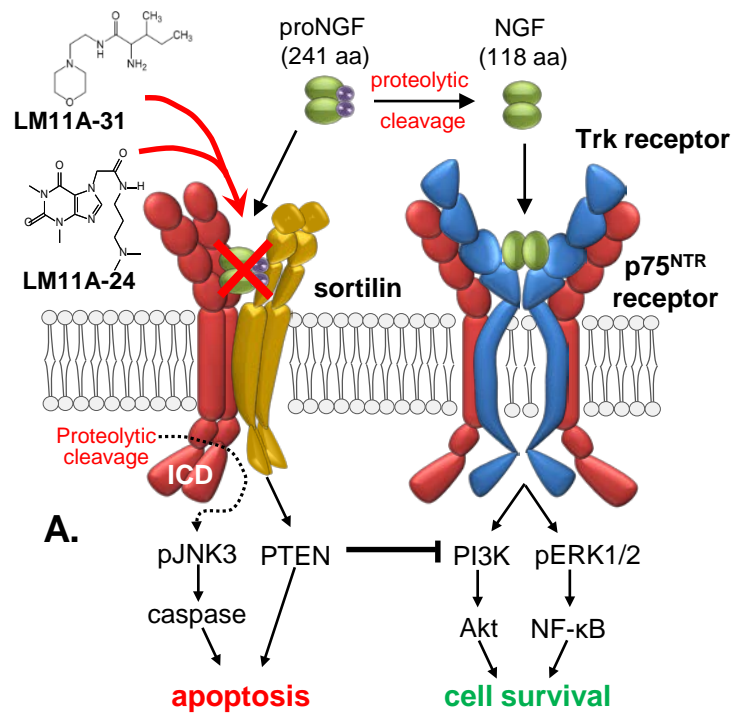
References

1. Fowler CJ, Griffiths D, de Groat WC. The neural control of micturition. *Nat Rev Neurosci.* 2008;9(6):453-466.
2. de Groat WC, Yoshimura N. Plasticity in reflex pathways to the lower urinary tract following spinal cord injury. *Exp Neurol.* 2012;235(1):123-132.
3. Fowler CJ, Panicker JN, Emmanuel A. *Pelvic organ dysfunction in neurological disease : clinical management and rehabilitation.* Cambridge: Cambridge University Press; 2010.
4. Merrill L, Gonzalez EJ, Girard BM, Vizzard MA. Receptors, channels, and signalling in the urothelial sensory system in the bladder. *Nature reviews Urology.* 2016;13(4):193-204.
5. McCarthy CJ, Zabbarova IV, Brumovsky PR, Roppolo JR, Gebhart GF, Kanai AJ. Spontaneous contractions evoke afferent nerve firing in mouse bladders with detrusor overactivity. *The Journal of urology.* 2009;181(3):1459-1466.
6. Ochodnický P, Cruz CD, Yoshimura N, Cruz F. Neurotrophins as regulators of urinary bladder function. *Nature reviews Urology.* 2012;9(11):628-637.
7. Lessmann V, Gottmann K, Malcangio M. Neurotrophin secretion: current facts and future prospects. *Prog Neurobiol.* 2003;69(5):341-374.
8. Teng KK, Felice S, Kim T, Hempstead BL. Understanding proneurotrophin actions: Recent advances and challenges. *Developmental neurobiology.* 2010;70(5):350-359.
9. Vaidyanathan S, Krishnan KR, Mansour P, Soni BM, McDicken I. p75 nerve growth factor receptor in the vesical urothelium of patients with neuropathic bladder: an immunohistochemical study. *Spinal Cord.* 1998;36(8):541-547.
10. Chao MV. Neurotrophins and their receptors: a convergence point for many signalling pathways. *Nat Rev Neurosci.* 2003;4(4):299-309.
11. Hass MR, Sato C, Kopan R, Zhao G. Presenilin: RIP and beyond. *Seminars in cell & developmental biology.* 2009;20(2):201-210.

12. Longo FM, Massa SM. Small-molecule modulation of neurotrophin receptors: a strategy for the treatment of neurological disease. *Nat Rev Drug Discov.* 2013;12(7):507-525.
13. Simmons DA, Belichenko NP, Ford EC, et al. A small molecule p75NTR ligand normalizes signalling and reduces Huntington's disease phenotypes in R6/2 and BACHD mice. *Hum Mol Genet.* 2016;25(22):4920-4938.
14. Tep C, Lim TH, Ko PO, et al. Oral administration of a small molecule targeted to block proNGF binding to p75 promotes myelin sparing and functional recovery after spinal cord injury. *J Neurosci.* 2013;33(2):397-410.
15. Ikeda Y, Fry C, Hayashi F, Stolz D, Griffiths D, Kanai A. Role of gap junctions in spontaneous activity of the rat bladder. *American journal of physiology Renal physiology.* 2007;293(4):F1018-1025.
16. Yu W, Ackert-Bicknell C, Larigakis JD, et al. Spontaneous voiding by mice reveals strain-specific lower urinary tract function to be a quantitative genetic trait. *American journal of physiology Renal physiology.* 2014;306(11):F1296-1307.
17. Gibon J, Kang MS, Aliaga A, et al. Towards the PET radiotracer for p75 neurotrophin receptor: [(11)C]LM11A-24 shows biological activity in vitro, but unfavorable ex vivo and in vivo profile. *Bioorg Med Chem.* 2016;24(19):4759-4765.
18. Harrington AW, Leiner B, Blechschmitt C, et al. Secreted proNGF is a pathophysiological death-inducing ligand after adult CNS injury. *Proceedings of the National Academy of Sciences of the United States of America.* 2004;101(16):6226-6230.
19. Klinger MB, Vizzard MA. Role of p75NTR in female rat urinary bladder with cyclophosphamide-induced cystitis. *American journal of physiology Renal physiology.* 2008;295(6):F1778-1789.
20. Kullmann FA, Clayton DR, Ruiz WG, et al. Urothelial proliferation and regeneration after spinal cord injury. *American journal of physiology Renal physiology.* 2017:ajprenal 00592 02016.

21. Klinger MB, Girard B, Vizzard MA. p75NTR expression in rat urinary bladder sensory neurons and spinal cord with cyclophosphamide-induced cystitis. *J Comp Neurol*. 2008;507(3):1379-1392.
22. Girard BM, Malley SE, Vizzard MA. Neurotrophin/receptor expression in urinary bladder of mice with overexpression of NGF in urothelium. *American journal of physiology Renal physiology*. 2011;300(2):F345-355.
23. Vizzard MA. Changes in urinary bladder neurotrophic factor mRNA and NGF protein following urinary bladder dysfunction. *Exp Neurol*. 2000;161(1):273-284.
24. Jornot L, Lacroix JS, Rochat T. Neuroendocrine cells of nasal mucosa are a cellular source of brain-derived neurotrophic factor. *Eur Respir J*. 2008;32(3):769-774.
25. Ochodnický P, Michel MB, Butter JJ, Seth J, Panicker JN, Michel MC. Bradykinin modulates spontaneous nerve growth factor production and stretch-induced ATP release in human urothelium. *Pharmacol Res*. 2013;70(1):147-154.
26. Vaidyanathan S, van Velzen D, Krishnan KR, et al. Nerve fibres in urothelium and submucosa of neuropathic urinary bladder: an immunohistochemical study with S-100 and neurofilament. *Paraplegia*. 1996;34(3):137-151.
27. Meeker R, Williams K. Dynamic nature of the p75 neurotrophin receptor in response to injury and disease. *J Neuroimmune Pharmacol*. 2014;9(5):615-628.
28. Park A. Alzheimer's From A New Angle. *Time*. 2016;187(6-7):64-68, 70.

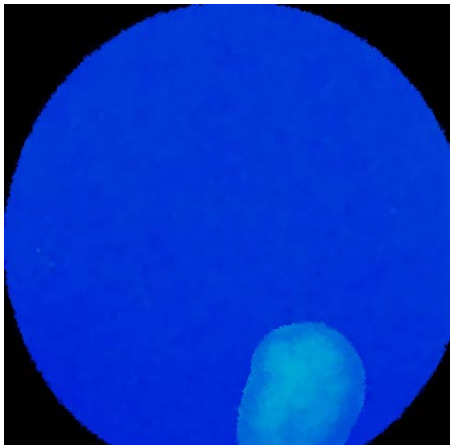
Figure 1



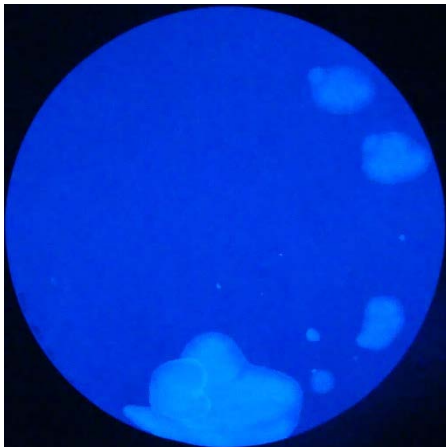
Neurotrophin receptors and known ligands	
Receptor	Ligand
p75 ^{NTR}	pro-NGF, -BDNF, -NT3, -NT4
TrkA	NGF
TrkB	BDNF/NT-4
TrkC	NT-3

Figure 2

A. SC intact
water gavage



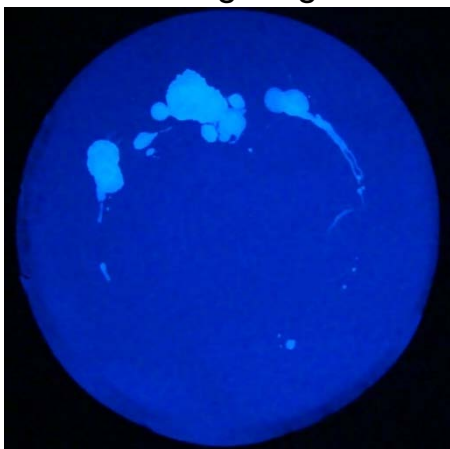
B. SC intact
LM11A-24 gavage



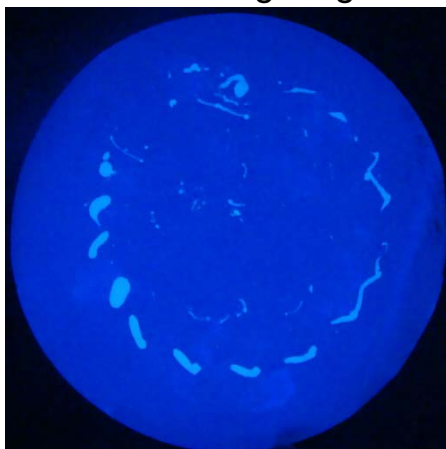
C. SC intact
LM11A-31 gavage



D. SCI 2 wks post injury
water gavage



E. SCI 2 wks post injury
LM11A-24 gavage



F. SCI 2 wks post injury
LM11A-31 gavage

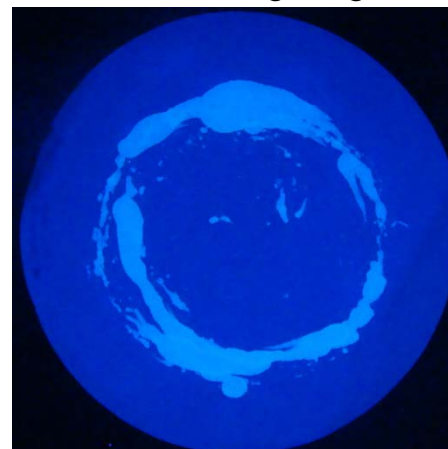
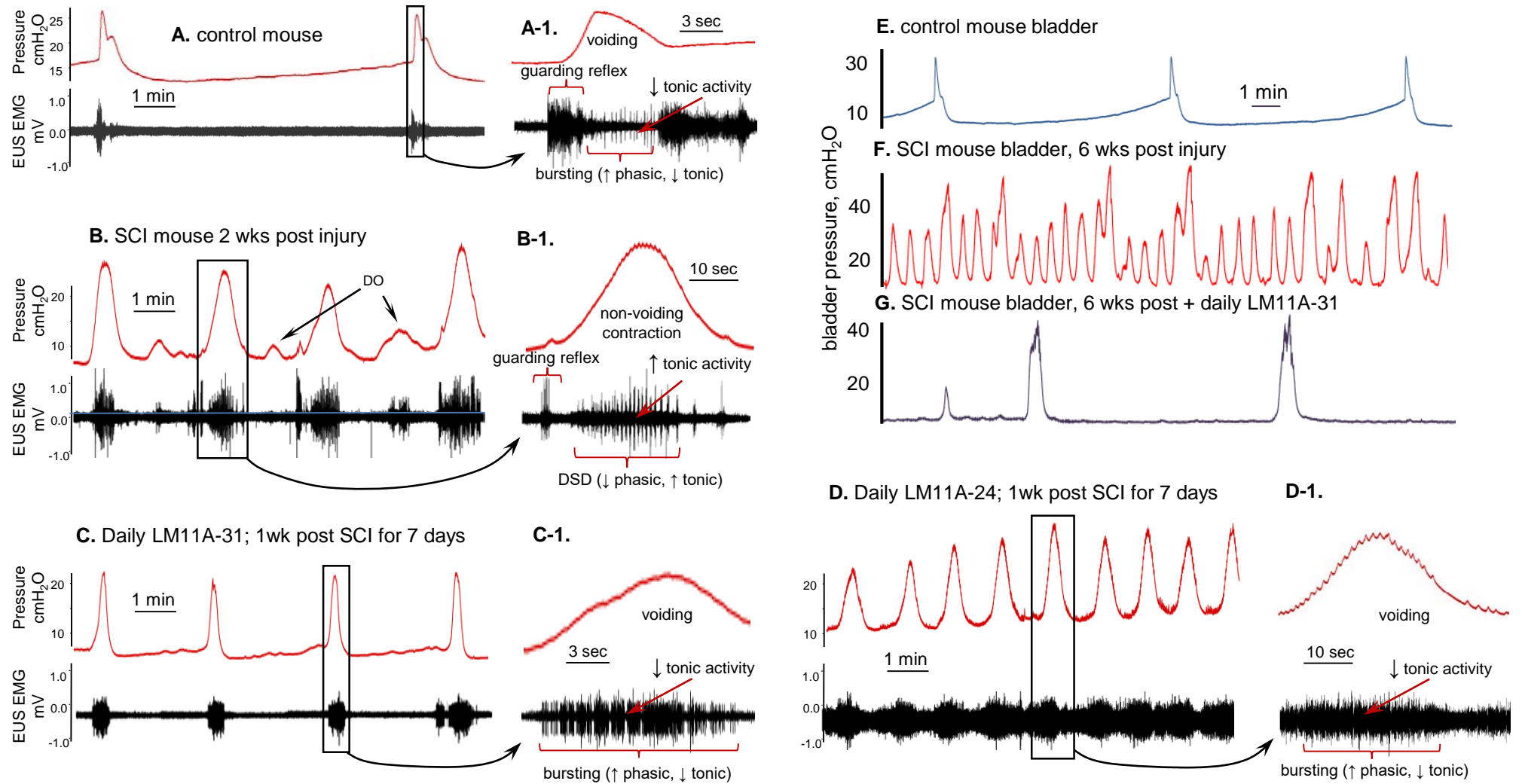


Figure 3



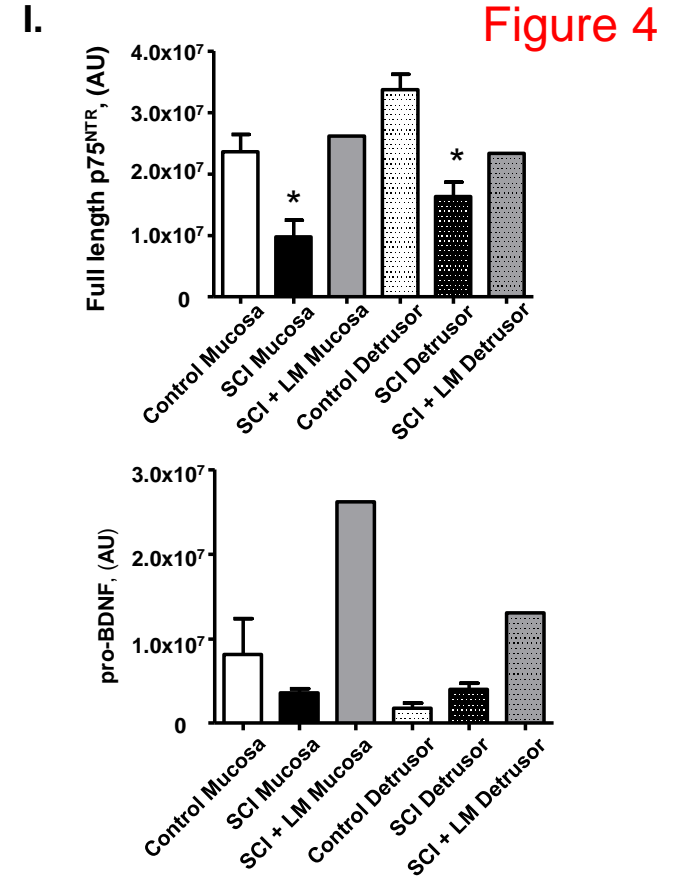
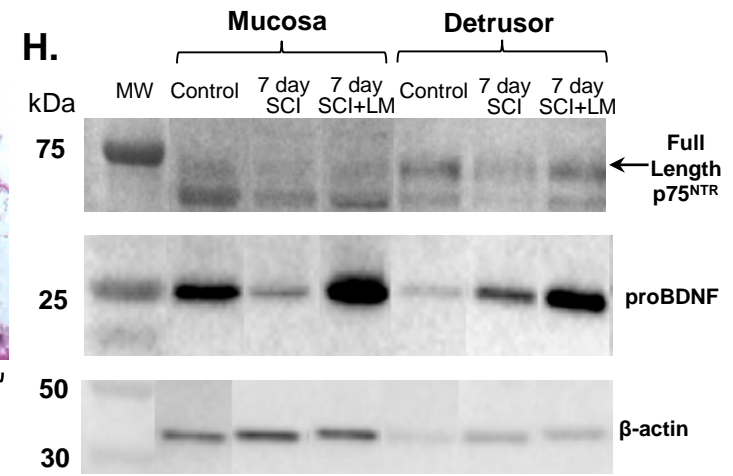
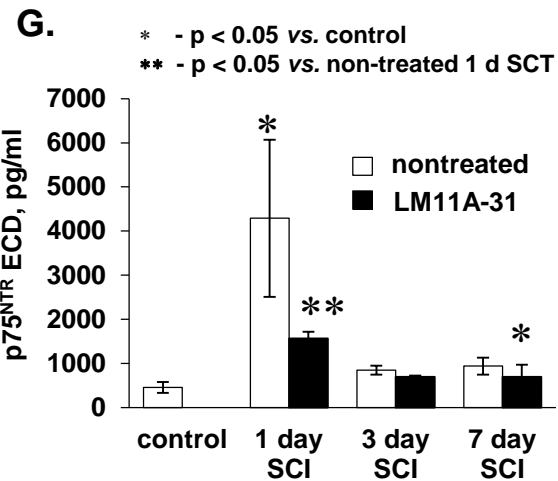
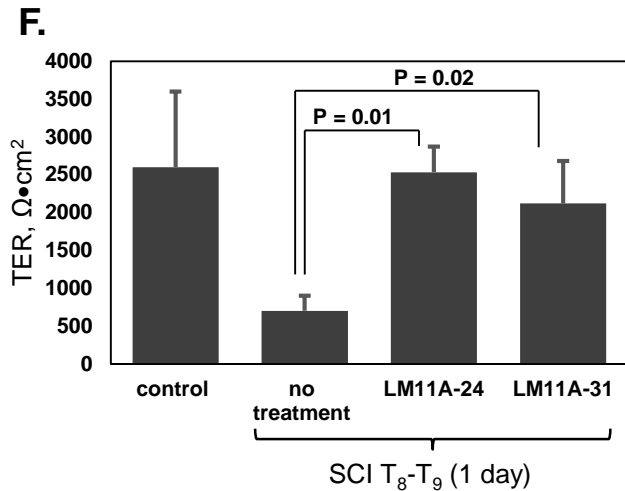
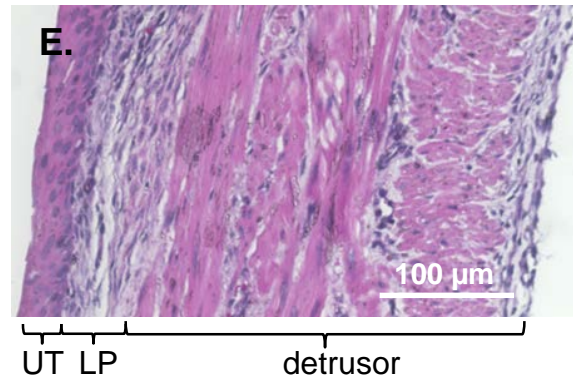
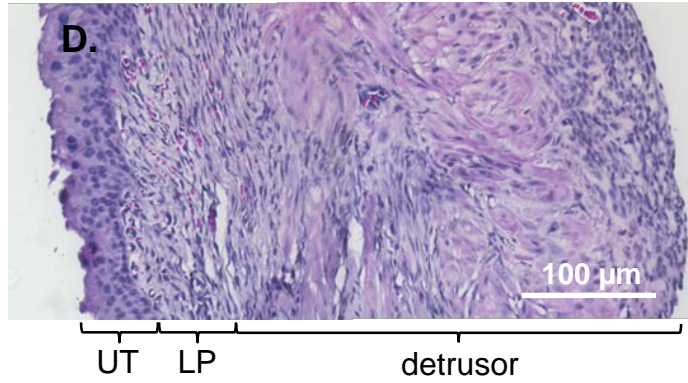
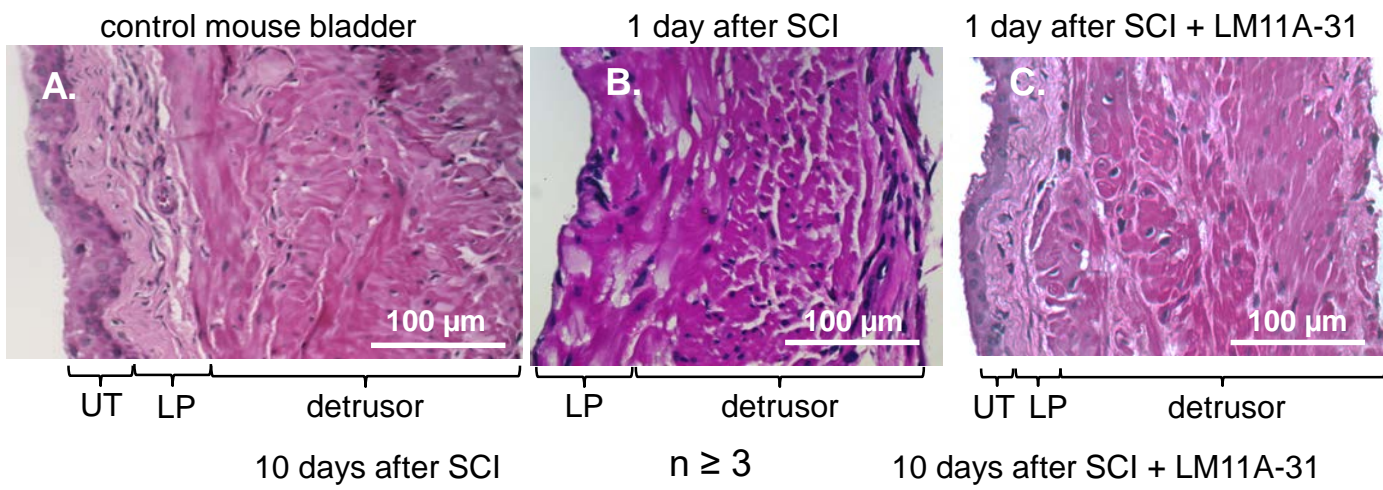
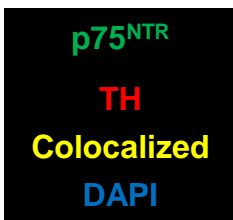
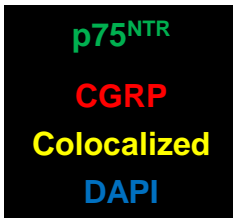


Figure 5

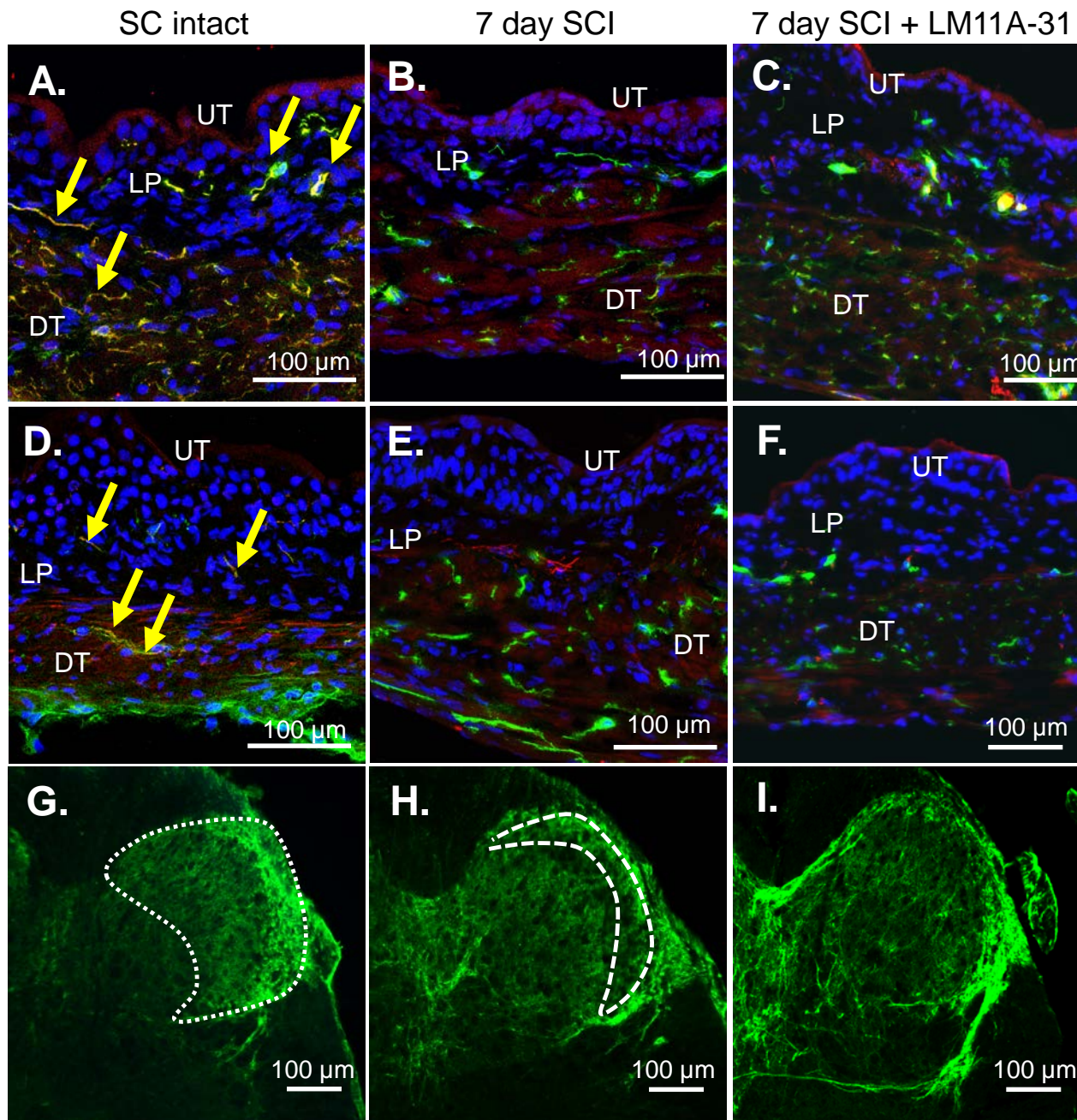
bladder wall



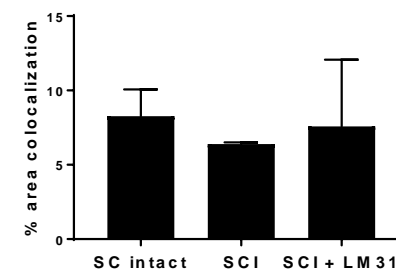
bladder wall



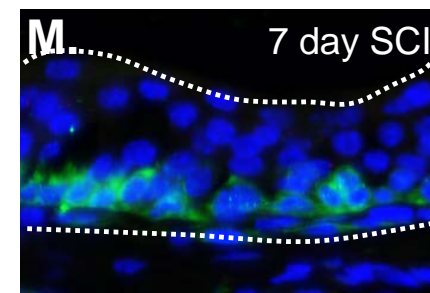
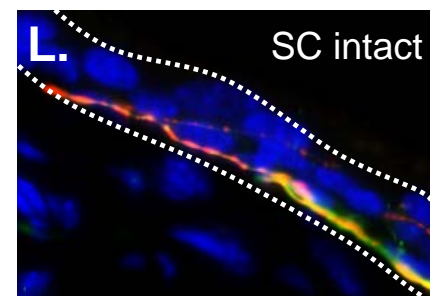
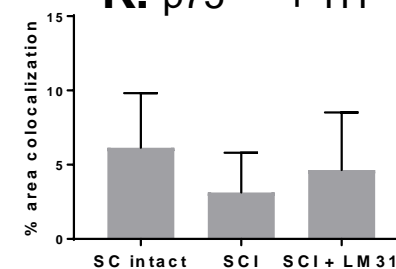
L₆ spinal cord



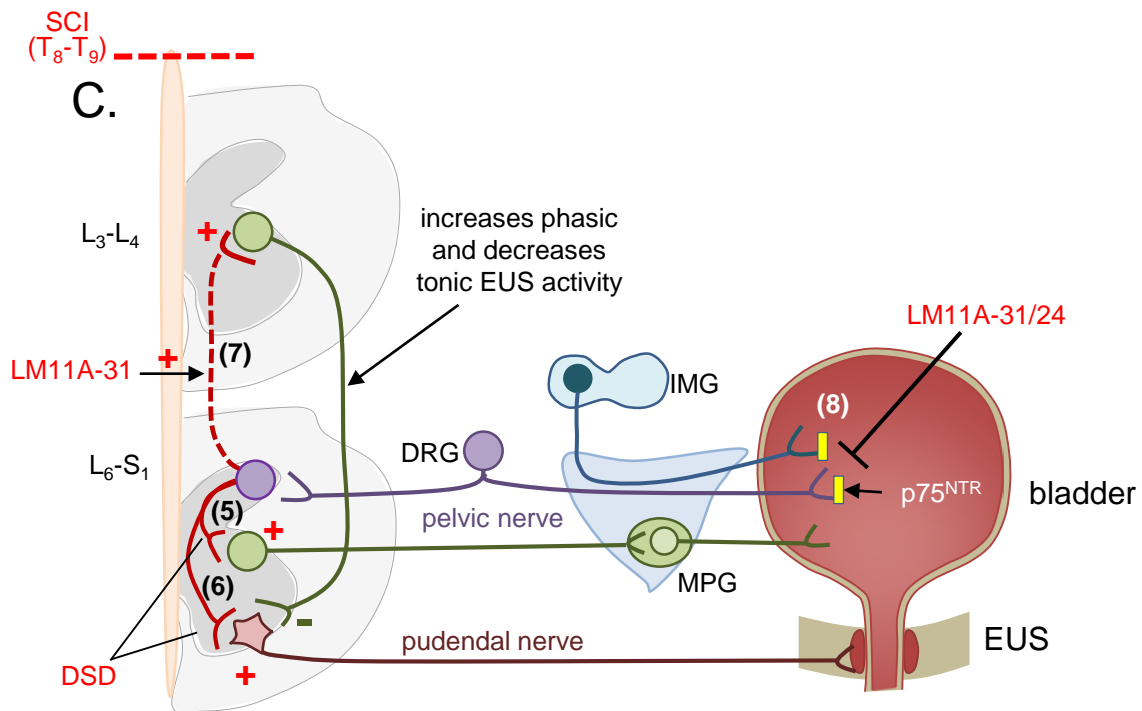
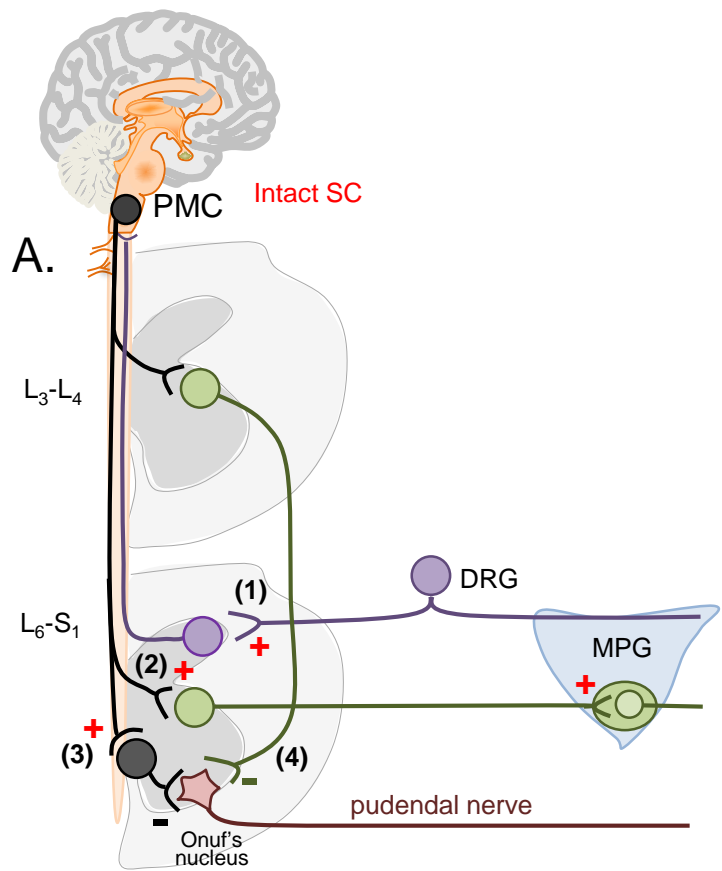
J. p75^{NTR} + CGRP



K. p75^{NTR} + TH



Supplemental Figure 6



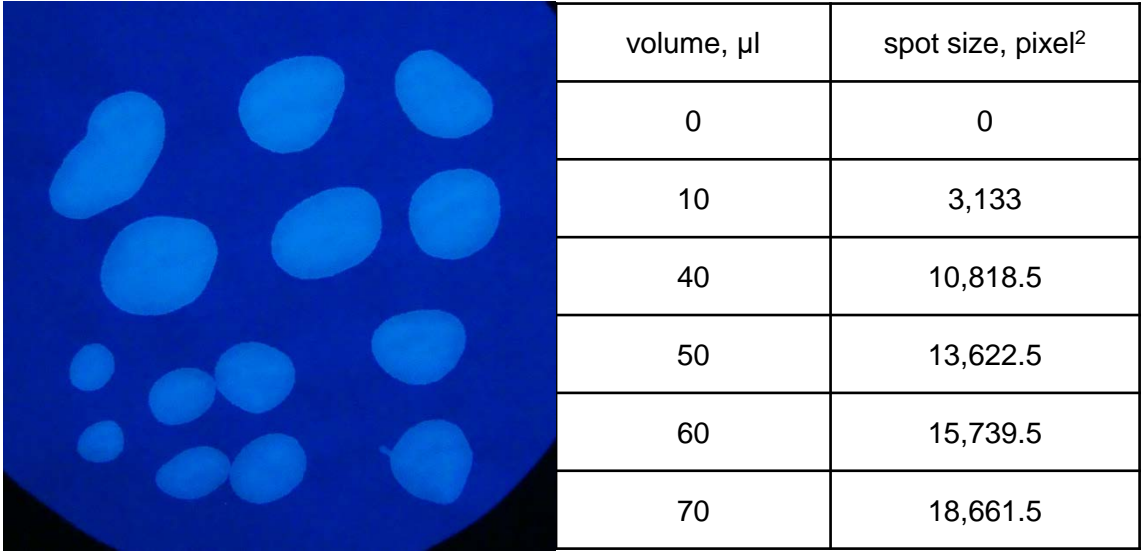
Supplemental Figure 7

Total volume, μ l

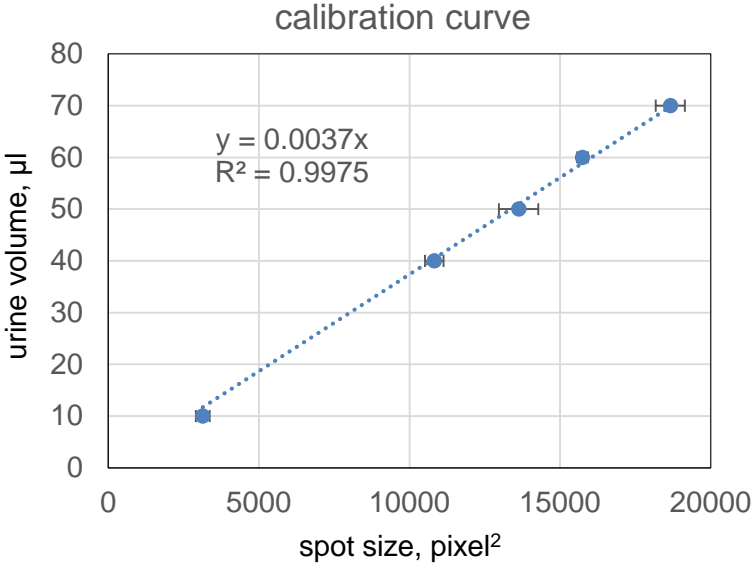
Spot Test Data	SC intact	SCI 2 wks	p
water	200 \pm 24	102 \pm 55	< 0.05
LM11A-24	241 \pm 70	109 \pm 40	< 0.05
LM11A-31	223 \pm 42	263 \pm 97*	

* - p < 0.05 compared to SCI with water

Supplemental
Figure 8



$\text{Volume } [\mu\text{l}] = 0.0037 \times \text{Spot Size } [\text{pixel}^2], R^2 = 0.9975$



Supplemental Figure 9

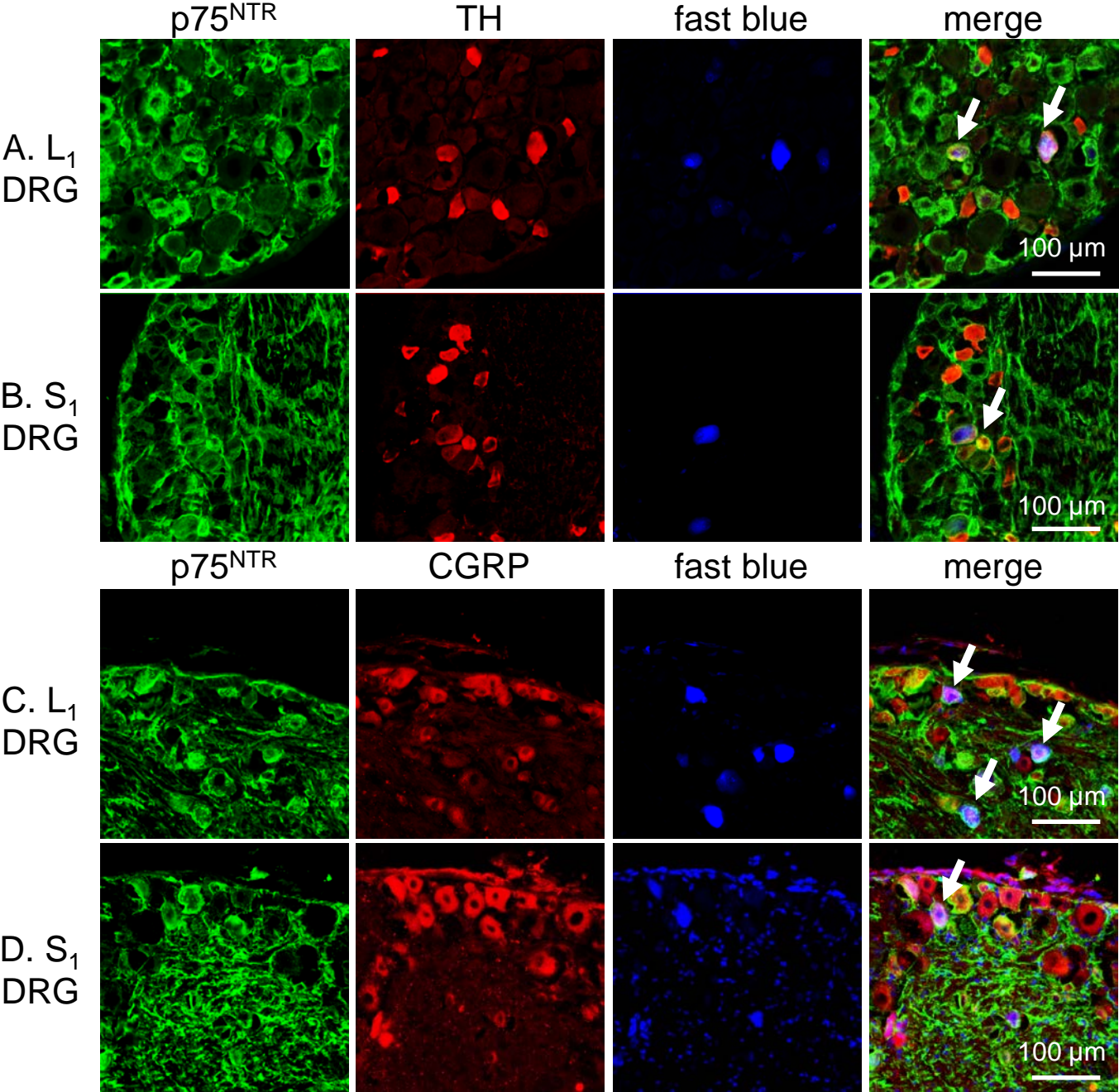
CMG Parameters	PT, cmH ₂ O	MVP, cmH ₂ O	BP, cmH ₂ O	ICI, sec	BC, μl/cmH ₂ O	NVC/10 min	VV, μl	RV, μl
control	8 ± 4	40 ± 10	4 ± 3	412 ± 24	15 ± 4	0	60 ± 8	9 ± 7
SCI, 2 wks	14 ± 6	24 ± 5	9 ± 5	197 ± 18*	7 ± 3*	6 ± 2*	30 ± 9*	400 ± 9*
SCI, 2 wks + LM11A-24	17 ± 1	32 ± 1	13 ± 2	211 ± 56*	9 ± 3	6 ± 2*	35 ± 8*	388 ± 18*
SCI, 2 wks + LM11A-31	7 ± 1	36 ± 2	4 ± 1	396 ± 37	22 ± 4	0.2 ± 0.4	64 ± 5	28 ± 8*
SCI, 6 wks	12 ± 8	52 ± 1	11 ± 2	43 ± 13*	7 ± 2*	13 ± 3*	186 ± 6*	550 ± 5*
SCI, 6 wks + LM11A-31	8 ± 2	49 ± 9	6 ± 2	510 ± 144	47 ± 10*	4 ± 2	85 ± 24	99 ± 8*

Supplemental
Figure 10

EMG Parameters	contraction duration, sec	voiding duration, sec	burst number	burst/sec
control	18.5 ± 1.6	5.3 ± 1	18 ± 4	3.3 ± 0.3
SCI, 2 wks	50.2 ± 3.7*	11.3 ± 4.7*	8 ± 4*	0.7 ± 0.2*
SCI, 2 wks + LM11A-31	16 ± 2	4 ± 0.7	15 ± 3	3.8 ± 0.9
SCI, 2 wks + LM11A-24	51.6 ± 3.5**	13.5 ± 3.2**	7.8 ± 0.8**	0.6 ± 0.1**

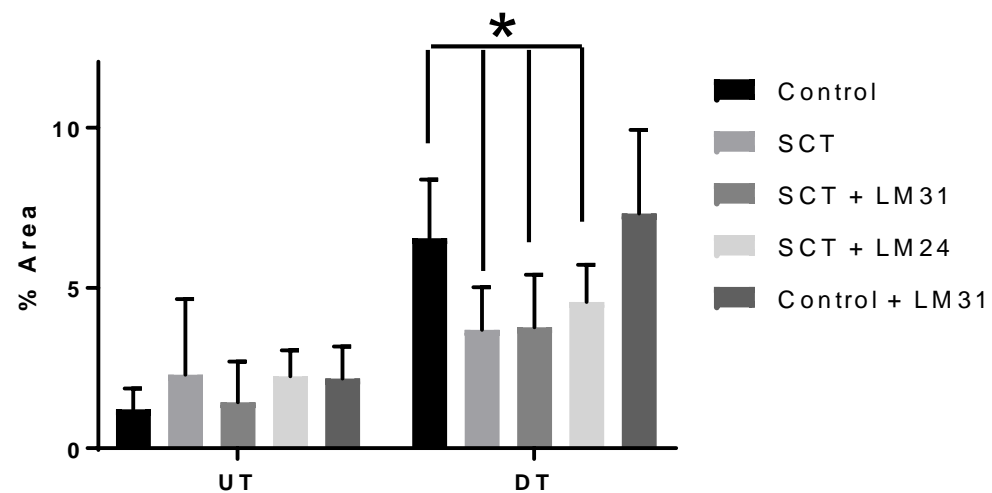
(*, ** -- p < 0.01 compared to both control and 2 weeks SCI with LM11A-31 therapy)

Supplemental
Figure 11

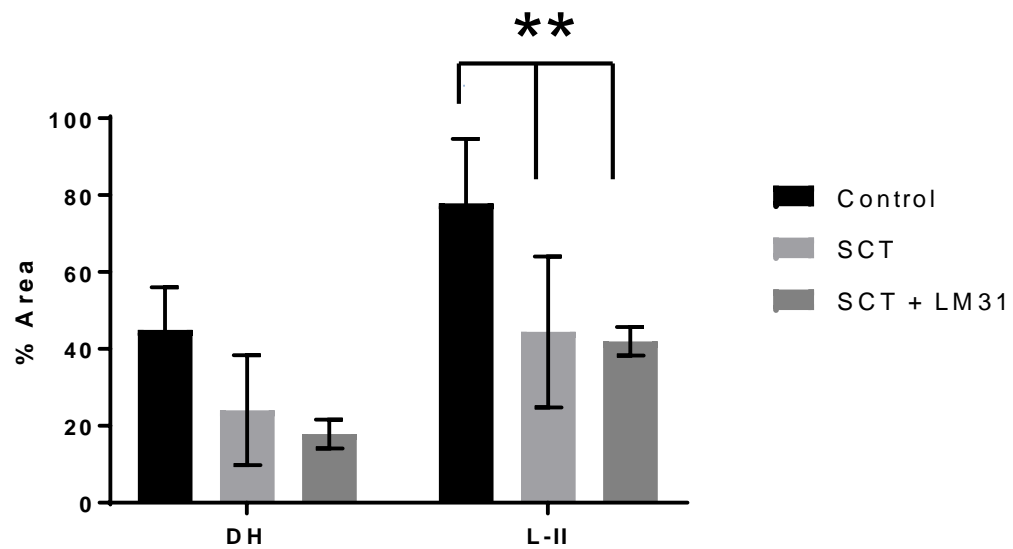


Supplemental
Figure 12

p75^{NTR} Bladder



p75^{NTR} L6S1 cord



Supplemental
Figure 13

Primary Antibodies (WB: western blot, IF: immunofluorescence)				
Antibody	Host	Concentration	Company	Catalogue number
p75 ^{NTR} intracellular domain	Rabbit	WB: 1:1000	Promega	G3231
p75 ^{NTR} extracellular domain	Goat	IF: 1:1000	Neuromics	GT15057
proNGF	Rabbit	WB: 1:1000	Life Technologies	OSN00007G
proBDNF	Mouse	WB: 1:500	Santa Cruz	sc-65514
β -actin	Rabbit	WB: 1:2000	Life Technologies	PA-183
Tyrosine hydroxylase	Rabbit	IF: 1:500	Abcam	ab112
CGRP	Rabbit	IF: 1:1000	Sigma	C8198
CGRP	Rabbit	IF: 1:2000	Immunostar	24112

Secondary Antibodies (WB: western blot, IF: immunofluorescence)				
Antibody	Host	Concentration	Company	Catalogue number
Anti-goat Alexafluor 488	Donkey	IF: 1:500	Life Technologies	A11055
Anti-rabbit Alexafluor 598	Donkey	IF: 1:500	Life Technologies	A21207
Anti-rabbit horseradish peroxidase (HRP) conjugate IgG	Donkey	WB: 1: 2000	GE Healthcare	NA934V
Anti-mouse HRP conjugate IgM	Mouse	WB: 1:2000	Santa Cruz	sc-2318
Anti-goat HRP conjugate IgG	Donkey	WB: 1: 2000	Novex	A16005